Cross comparison of surface slope and height optical metrology with a super-polished plane Si mirror

Nikolay A. Artemiev,*[a] Daniel J. Merthe,[a] Daniele Cocco,[b] Nicholas Kelez,[b] Thomas J. McCarville,[c] Michael J. Pivovaroff,[c] David W. Rich,[b] James L. Turner,[b] Wayne R. McKinney,[a] and Valeriy V. Yashchuk[a]

[a] Advanced Light Source, Lawrence Berkeley National Laboratory, Berkeley, CA 94720, USA
[b] SLAC National Accelerator Laboratory, 2575 Sand Hill Road, Menlo Park, CA 94025, USA
[c] Lawrence Livermore National Laboratory 7000 East Ave., Livermore, CA 94550, USA

ABSTRACT

We report on a cross-comparison of low-spatial-frequency surface slope and height metrology with a super-polished flat X-ray mirror Si substrate fabricated for the Stanford Linear Accelerator Center Linac Coherent Light Source hard X-ray mirror system HOMS-3. The substrate with overall dimensions of 450 × 30 × 50 mm^3 was specified to have a radius of curvature between 150 km and 195 km with a residual (after subtraction of the best-fit cylinder) slope variation on the level of 0.1 μrad rms, when measured in the tangential direction over a clear aperture of 380 × 5 mm^2. Surface slope metrology with an accuracy of better than 60 nrad rms was performed with an upgraded long trace profiler LTP-II and an auto-collimator-based developmental LTP (DLTP). The instruments are available at Advanced Light Source optical metrology laboratory. Surface figure in the height domain was characterized at the Lawrence Livermore National Laboratory X-ray science and technology group with a large field-of-view ZYGO™ (12 in) interferometer. The error of the interferometric measurement is estimated to be approximately 0.5 nm rms. We describe in detail the experimental methods and techniques that achieved state-of-the-art metrology with the super-high quality optic under test. We also discuss the relation between surface slope and height metrology and the principle problems of their cross-comparison. We show that with some precautions cross comparison can be made reliably, providing supplemental information on surface figure quality.

Keywords: X-ray optics, synchrotron radiation, metrology of X-ray optics, long trace profiler, optical interferometry, super-polished flat X-ray mirror, optical metrology, wave-front preserving optics

1. INTRODUCTION

The Linac Coherent Light Source (LCLS)[1] is currently in operation at the Stanford Linear Accelerator Center (SLAC). This is the first Free Electron Laser (FEL) facility in the world generating coherent X-ray light in the 0.827 to 8.27 keV photon energy region (0.15 − 1.5 nm wavelength region). The unique properties of the FEL beam such as brightness, coherence and time resolution enable considerable advances in physics, chemistry, biology, and material science. To preserve brightness and coherence of the LCLS and deliver the beam over distances of hundreds of meters, optics of the highest available quality with respect to surface figure and surface roughness are needed. Moreover, in addition to generating a coherent X-ray beam, the electron beam also emits spontaneous radiation. This spontaneous radiation has a broad spectrum extending up to the very hard X-ray region and has a total power approximately one order of magnitude higher than the FEL power. This spontaneous background radiation must be filtered out before the pulse enters an experimental station. A pair of flat parallel grazing incidence mirrors, with a clear aperture that matches the FEL beam size, spatially filters out the large divergent spontaneous background and effectively cuts off the high-energy components of the spontaneous radiation. This pair of mirrors constitutes the Hard X-ray Offset Mirror System (HOMS), which is installed approximately 100 m downstream of the exit of the undulator at the LCLS.[2]

*NArtemiev@lbl.gov; phone 1 510 495-2159; fax 1 510 495-2719; http://opticalmetrology.lbl.gov

In order to minimally disturb the FEL pulse wave front, the surface of these mirrors must have the highest possible figure and finish quality. In general, the root mean square (rms) height error goal for the optics' surfaces is given by the Maréchal criterion:[3]

$$\Delta h \le \frac{\lambda}{14\sqrt{N}\,2\theta} \tag{1}$$

where θ is the grazing incidence angle and N is number of optical elements in the system.[4] Taking the highest photon energy of 25 keV, three optical elements in the system and a 1.3 mrad[2] angle of incidence we get an upper bound for the height errors on all of the reflecting surfaces:

$$\Delta h \le 0.7 nm \text{ (rms)} \tag{2}$$

Such stringent requirements are needed for brightness and coherence preservation of Free Electron Laser X-ray light sources and necessitate extending the capabilities of X-ray optics.[5-7] This also demands new optical metrology methods at the level of and surpassing 0.1 μrad rms. The best slope measuring instruments available at synchrotron radiation sources worldwide, such as the Nanometer Optical Component Measuring Machines (NOM) at Helmholtz Zentrum Berlin (HZB)/BESSY-II[8] (Germany) and at the Diamond Light Source[9] (UK), as well as Long Trace Profilers (LTP) at SPring-8[10] (Japan), ESRF,[11, 12] SOLEIL[13, 14] (France), and the Advanced Light Source[15-17] (ALS, U.S.A.) approach the required level of accuracy.

The dimensions of the HOMS-3 mirror substrate under discussion here are 450 mm × 30 mm × 60 mm with a clear aperture of 380 mm × 5 mm. In the tangential direction, the polishing was specified to have a residual slope variation lower than 0.1 μrad rms and a radius of curvature 150 km ≤ R ≤ 195 km over the clear aperture, and 0.63 μrad rms over the whole surface of the substrate. Specification for the surface error along the sagittal direction is significantly looser, < 2 μrad rms due to so-called "forgiveness factor". The mirror was also specified to have a residual shape error, after subtraction of a best-fit sphere, of less than 1 nm rms within the clear aperture. The slope and height error specifications for the surface figure are especially crucial in meeting the requirements for coherence preservation of the LCLS coherent beam.

The HOMS-3 substrate was measured at Lawrence Livermore National Laboratory (LLNL) using a Zygo™ interferometer with an aperture of twelve inches[18] and at the optical metrology laboratory (OML) of the ALS of Lawrence Berkeley National Laboratory (LBNL) by the upgraded second generation LTP-II[15] and the autocollimator based Developmental Long Trace Profiler (DLTP).[16] While the ALS LTP-II and the DLTP measure surface slope, the LLNL 12-in interferometer measures surface height.

In the case of synchrotron optics the slope error profile is a measure of the surface quality used by beamline designers for ray-trace simulations. The height error profile is necessary for calculations of coherent beam wave front distortions, e.g., in the case of the FEL optics. The height profile measurements are also used by optical manufacturer to control the polishing process.

In this article we discuss metrological measurements of the new HOMS-3 mirror substrate performed with different instruments and make a cross comparison of the results in the slope and height domains. In Secs. 2 and 3 we describe surface metrology in the height and slope domains and discuss methods which allow us to effectively suppress random and systematic errors of the measurements. In Sec. 4 we present methods of transforming a surface slope profile into a height profile and discuss errors associated with the integration. In Sec. 5 we apply these integration techniques to compare the metrology results obtained with different instruments. Finally we demonstrate that current state-of-the-art surface optical metrology is capable of precise characterization of surface figure of high quality x-ray optics designed and fabricated for FEL applications.

2. SURFACE METROLOGY IN THE HEIGHT DOMAIN

The surface figure of the HOMS-3 Si substrate was measured by full-aperture interferometry at LLNL, using a Zygo Mark II,™ 12-in-aperture phase-shifting Fizeau-type interferometer, operating at the He-Ne wavelength of 633 nm. A calibrated transmission flat was used as a reference surface.[18] Fig. 1 schematically illustrates the interferometric measurements.

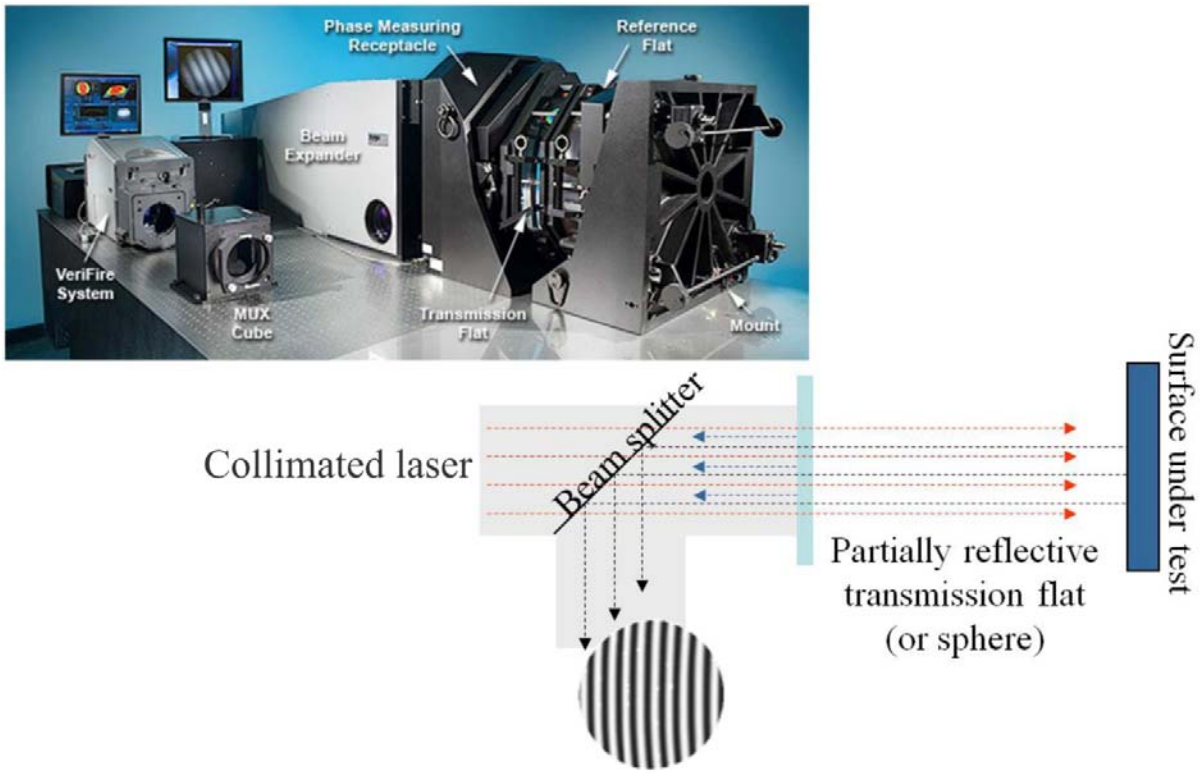

Figure 1: Surface height measurements with the Fizeau interferometer.

A collimated laser beam is sent to a reference flat reflecting a small fraction back and transmitting most of the beam to the surface under test (SUT). The laser beam comes back to the reference flat after being reflected by the SUT and interferes with the part of the beam reflected by the reference flat creating an interferogram recorded by a CCD. Deviations from straight fringe lines correspond to modification of the laser wave front due to imperfections, astigmatism etc., of the SUT. The CCD detector of the interferometer is 540 pixels across corresponding to an effective pixel size of 0.56 mm.

The result obtained at the LLNL, after subtraction of the best fitting sphere and stitching three overlapping interferograms, is presented in Fig. 2.

The precision of the height measurements with the interferometer is approximately ±0.1 to ±0.2 nanometers. This is demonstrated by taking repeated measurements of the same surface, and observing the statistical variation of the results. The absolute accuracy of the height measurements depends on how well the reference flat is calibrated. An absolute calibration of the reference flat was performed with the accuracy of better than 1 nm.[18]

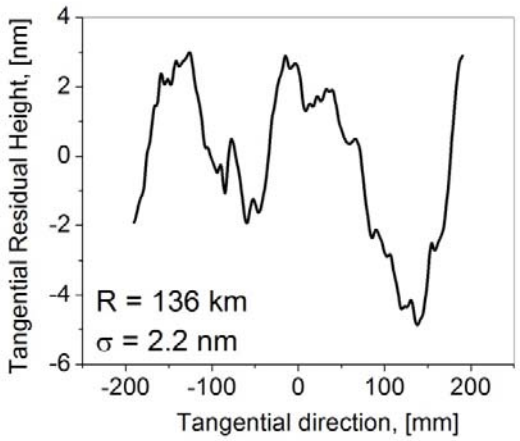

Figure 2: Residual surface height error after best sphere subtraction as measured at LLNL. Residual shape error is 2.5 nm rms over the whole surface and 1.9 nm rms over 380 mm clear aperture.

3. SURFACE METROLOGY IN THE SLOPE DOMAIN

The HOMS-3 substrate was measured at the ALS OML, where two direct slope measuring instruments, LTP-II[15, 17] and DLTP,[16] were used.

3.1 LTP-II measurement

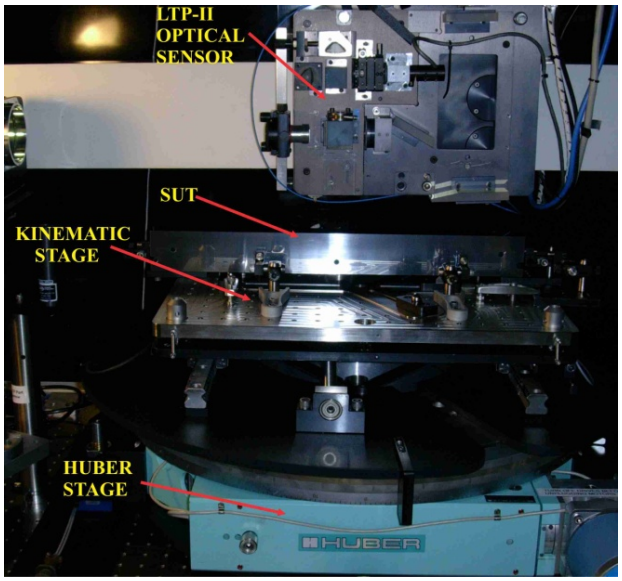

Figure 3: Experimental arrangement of the LTP-II measurements with the super-polished flat x-ray mirror Si substrate fabricated for the LCLS HOMS project (Mirror #3). The substrate under measurement is placed on an automated rotating, flipping, and aligning (ARFA) system.[19] With the ARFA system, high precision slope measurements with significant suppression of instrumental errors due to systematic effects, set-up drifts, and random noise become possible.[15, 17, 19, 20]

The substrate was measured along one central tangential trace of 440 mm. Figure 3 depicts the experimental arrangement of the LTP-II measurements. The measurement procedure used is the same as discussed in Ref.[19]

The expected surface figure distortion of the HOMS-3 single crystal silicon substrate (with an assumed Young's modulus of 131 GPa and a density of 2.3 g/cm^3) due to gravity is of the same order of magnitude as the specified residual surface slope error. Therefore for the slope measurements, the mirror was installed oriented face up on two supports (a cylinder and a ball) displaced symmetrically about the substrate's geometrical center. The spacing between the supports was (251 ± 0.5) mm corresponding to the slope-minimizing Bessel points, thereby reducing the surface slope error due to gravity sag down to 60 nrad rms. Thus the effect of gravity sag can be accurately predicted and removed from the measured data.

In order to provide the required accuracy of the slope metrology of ≤ 100 nrad, a single slope profile measurement performed with the LTP-II consisted of 32 scans, which were averaged. The first 16 scans were split into 2 runs, each with different orientations (unflipped and flipped) of the SUT with respect to the LTP translation system. Each run consisted of 8 sequential scans performed in the forward (F) and backward (B) scanning directions according to the optimal strategy F-B-B-F-B-F-F-B (see Ref.[20]). In order to be certain that the measured slope profile accurately represents the SUT, rather than LTP-II systematic errors, two additional runs (with the SUT flipped and unflipped) were carried out with the SUT shifted longitudinally by 31.5 mm. This is the maximum practically possible shift with the ARFA system while maintaining the Bessel point supports for the SUT.

In the course of the LTP-II measurements, the direction of the scans was automatically controlled by the LTP software. Flipping of the SUT between the LTP runs was performed with an automated rotating, flipping, and aligning (ARFA) system,[19] when the LTP was at rest. After each reset of the SUT with the ARFA system, we checked the preservation of the correct tangential and sagittal position of the next scanning trace.

The described measurement procedure effectively suppresses errors due to drifts and systematic effects.[15, 20] Note that in the course of the LTP-II measurements we did not make additional runs with different tilts of the SUT that would decrease the possible systematic error due to non-ideality of the LTP optical elements. As we have verified in a dedicated calibration experiment, in the case of ALS LTP-II measurements with flat optics, this systematic error is negligibly small. Nevertheless, after flipping and shifting, the SUT tilt with respect to the LTP was actually slightly (but significantly more than the total angular range of the measurements) changed; and averaging over the additional runs provided suppression of this kind of error, if any existed.

3.2 DLTP measurement

In addition to the LTP-II measurements, we performed similar surface slope metrology of the HOMS-3 mirror with the DLTP[16] also available at the ALS OML. Thirty two DLTP scans were split into two runs with two different orientations (unflipped and flipped) of the SUT with respect to the DLTP translation system and two runs with slightly different tangential tilts of the SUT. Each run consisted of 8 sequential scans performed in the forward (F) and backward (B) scanning directions according to the optimal strategy F-B-B-F-B-F-F-B. The runs with different tangential tilts (-140 μrad for the unflipped SUT and +160 μrad for the flipped SUT) were carried out in order to suppress the contribution of a systematic error with a period of about 280 μrad, characteristic of this DLTP. Note that in the course of the DLTP measurements the SUT rested on a few clean tissues placed on an aluminum plate rather than on the Bessel point supports.

4. AVERAGING OF LTP AND DLTP MEASUREMENTS

Figure 4 a) presents the resulting residual slope profiles measured with the LTP-II (black solid curve) and DLTP (red dashed curve), obtained by averaging over all runs and subtracting the best fit line.

In the tangential direction, the substrate has a plane shape with a radius of curvature of the best fit cylindrical figure of 108.5 km and 126.9 km, as measured with the LTP-II and DLTP, respectively. The rms residual slope variations are found to be 149 nrad and 167 nrad. These values correspond to the clear aperture of the mirror surface. The difference of

the rms slope variation can be explained as a manifestation of the different lateral resolution of the instruments. Note that the LTP-II measurements were performed with an increment of 1 mm; whereas the increment of the DLTP scans was 0.2 mm.

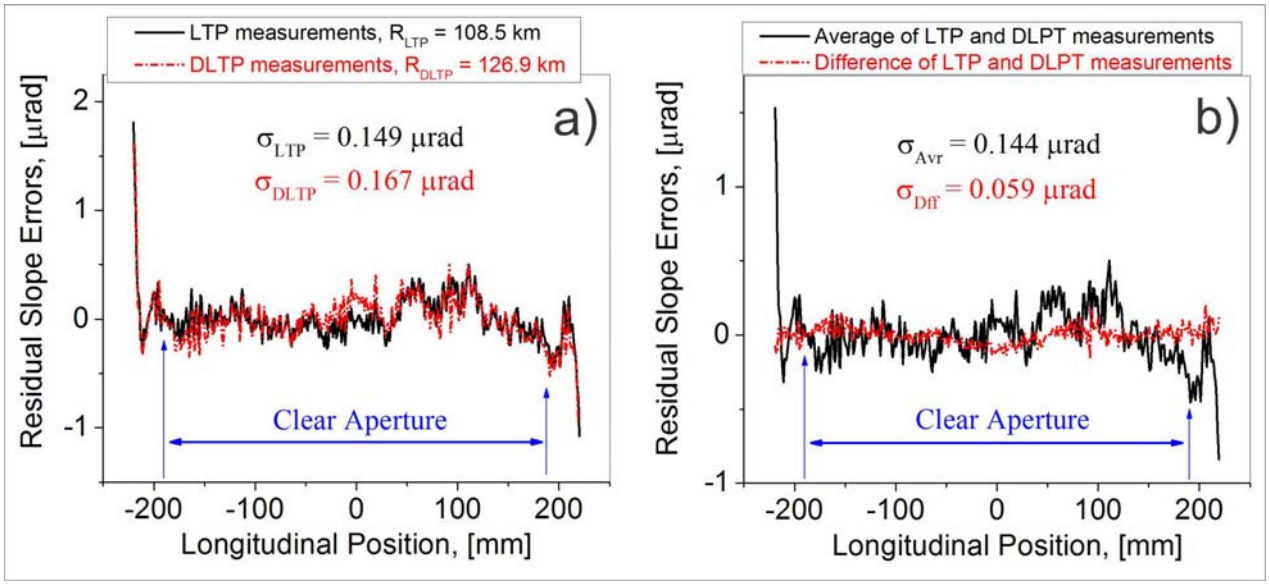

Figure 4: a) Resulting residual slope profiles of the mirror substrate measured with the LTP-II (black solid curve) and the DLTP (red dashed curve) along the tangential direction, and centered along the sagittal direction. The measured substrate has a cylindrical shape appearing as a line in the slope domain. b) Resulting residual slope profiles of the mirror substrate averaged over the LTP-II and DLTP measurements (black solid curve) and a half of the difference of the LTP-II and DLTP measurements (red dashed curve). Note that the systematic variations in the difference profile are effectively averaged out in the averaged residual slope profile. The corresponding residual slope variations and the radii of the subtracted best-fit cylindrical surfaces for the clear aperture of the mirror are shown in the plots. The surface parameters were evaluated over the mirror clear aperture.

Note that there is no noticeable residual slope perturbation due to the gravity sag effect that should be seen as a difference between the LTP-II and DLTP measurements due to the difference in the SUT mounting.

In order to understand the magnitude of the instrumental error in these measurements, different cross-checks of the performed runs have been made in the same manner as in Ref.[19] The rms measurement error for a single run is found to be about $\sigma_{err} \cong 80$ nrad. The estimated rms error of the resulting measurements is about 40-60 nrad.

To average out systematic errors of LTP and DLTP half of the sum of the two residual slope profiles is computed as follows:

$$S_{Avr} = \frac{1}{2}((\alpha_0 + E_{LTP}) + (\alpha_0 + E_{DLTP})) = \alpha_0 + \frac{E_{LTP} + E_{DLTP}}{2}, \quad (3)$$

where S_{Avr} is the averaged residual slope profile, α_0 is slope profile of the SUT, and E_{LTP} and E_{DLTP} are the systematic errors of the LTP and the DLTP respectively. In such a way we decrease by a factor of two the contributions of uncorrelated instrumental systematic errors into the final residual slope profile. The instruments are based on different optical schemes and optical sensors, and are located in two different optical hutches. This suggests that the LTP and the DLTP have independent and uncorrelated systematic errors. By taking the difference between the residual slope profiles

measured with the LTP and the DLTP we exclude the shape of the SUT and effectively reveal the suppressed systematic errors:

$$S_{Err} = \frac{1}{2}((\alpha_0 + E_{LTP}) - (\alpha_0 + E_{DLTP})) = \frac{E_{LTP} - E_{DLTP}}{2} \quad (4)$$

The total result of the slope measurements is presented in Fig. 4b as residual slopes, and the average slope profile combining both the LTP-II and the DLTP measurements (Fig. 4a) along with half the difference of the LTP and the DLTP slope profiles. The corresponding rms residual slope errors also suggest an accuracy of the performed metrology below 60 nrad.[19] In order to merge the two data sets obtained with the LTP-II and the DLTP, the DLTP data were averaged over each 5 sequential points using the Savitzky-Golay method[21] in order to correspond to the 1 mm increment of the data obtained with the LTP-II.

5. INTEGRATION OF SLOPE DISTRIBUTIONS INTO HEIGHT DISTRIBUTIONS

The simplest way to transfer surface slope data into height data is to apply a Riemann summation. If we have a set of slope measurements $s(x_1)$, $s(x_2)$, …, $s(x_N)$, for positions x_1, x_2, …, x_N on the SUT with an increment Δx, the height calculated as a Riemann sum at a point x_n is given by

$$h(x_n) \equiv \int_a^{x_n} s(x')dx' \approx \Delta x \sum_{m=1}^{n} s(x_m), \quad (5)$$

where a is a constant. In this case, if the slope measurement at position x_m has an error ε_m, then the corresponding height error is

$$\gamma(x_n) = \Delta x \sum_{m=1}^{n} \varepsilon(x_m). \quad (6)$$

If we assume these slope errors to be random, independent and identically distributed, with zero mean and variance σ_ε^2, then the variances transform in a similar way,

$$\sigma_{\gamma n}^2 = \Delta x^2 \sum_{m=1}^{n} \sigma_{\varepsilon m}^2 = n\Delta x^2 \sigma_\varepsilon^2, \quad (7)$$

where $\sigma_{\gamma n}^2$ is the variance of the height error at point x_n, and $\sigma_{\varepsilon m}^2 = \sigma_\varepsilon^2$ is the variance of slope error, which is the same for every point x_m. Evidently, the random error appears to accumulate on one end of the SUT. This is therefore an undesirable method of generating the height data. Note that the trapezoid rule, Simpson's rule and other Newton-Cotes approximate integration techniques suffer essentially the same drawback as the Riemann summation.

To avoid this problem, a common alternative method is to perform the integration in the frequency domain (see, e.g., Ref.[22]). Let C_k be the discrete Fourier transform (DFT) of the slope data,

$$s(x_n) = \sum_{k=0}^{N-1} C_k \exp(i2\pi kn/N) \Leftrightarrow C_k = \frac{1}{N}\sum_{n=1}^{N} s(x_n) \exp(-i2\pi kn/N). \quad (8)$$

Then, from the properties of Fourier transforms, the height data is given by

$$h(x_n) = \left(\frac{N\Delta x}{2\pi i}\right)\left[\sum_{k=1}^{\lfloor N/2 \rfloor} \frac{C_k}{k} \exp(i2\pi kn/N) + \sum_{k=\lceil N/2 \rceil}^{N-1} \frac{C_k}{k-N} \exp(i2\pi kn/N)\right] \quad (9)$$

to within a constant offset, where $\lfloor N/2 \rfloor$ denote floor and ceiling functions, respectively. This integration scheme assumes that the surface slope as a function of position contains no frequencies higher than half the sampling frequency. It can be shown that this calculation of height from slope is equivalent to the one step transformation,

$$h(x_n) = \Delta x \sum_{m=1}^{N} s(x_m)\Phi(n-m, N), \quad (10)$$

where $\Phi(u, N)$ is the antiderivative of the Dirichlet kernel,

$$\Phi(u,N) \equiv \int_0^u \frac{\sin(\pi u')}{N\sin(\pi u'/N)}\,du'. \tag{11}$$

If as above, we assume the slope measurement errors to be random and independent and identically distributed, then the variance of the computed height value at the point x_n is

$$\sigma_{\gamma n}^2 = \Delta x^2 \sigma_\varepsilon^2 \sum_{m=0}^{N-1} \Phi(m,N)^2. \tag{12}$$

Inspection of the function $\Phi(u,N)$ shows that $\Phi(0,N) = 0$ and $\Phi(0 < m < N, N) \approx \pm 1/2$. Therefore, the variance becomes approximately,

$$\sigma_{\gamma n}^2 \approx \frac{N-1}{4} \Delta x^2 \sigma_\varepsilon^2. \tag{13}$$

This variance is about half the average variance that one would incur with the Riemann sum method, and is moreover independent of the position x_n of the data point.

6. COMPARISON OF LLNL INTERFEROMETRIC DATA AND OML SLOPE INTEGRATED DATA

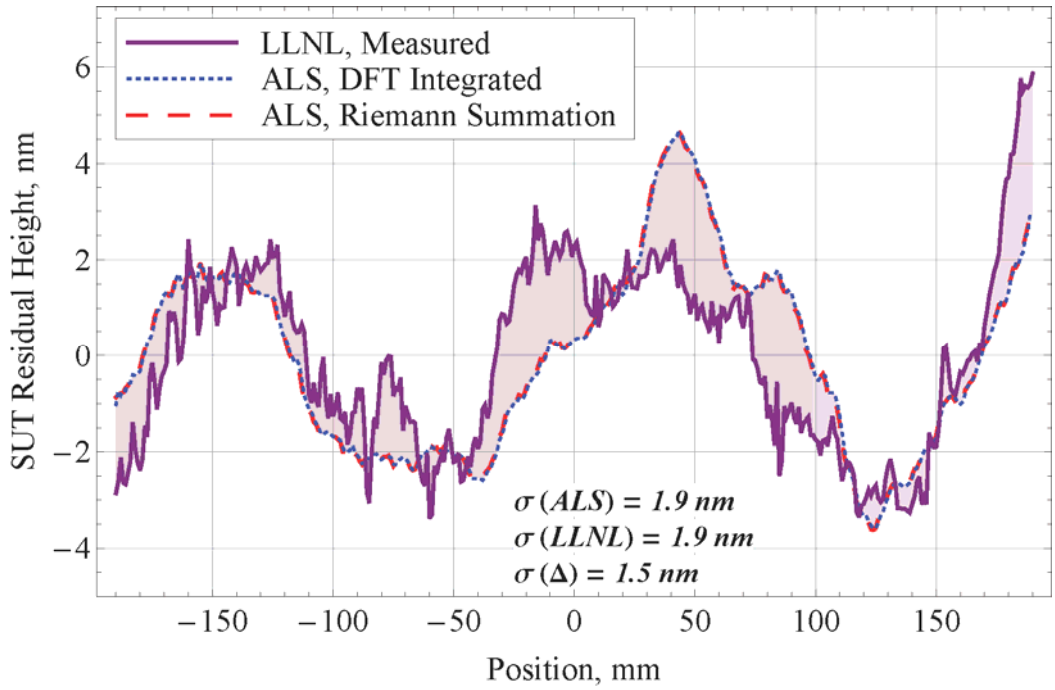

Figure 5: Comparison of measured residual height to residual height generated from slope data. Quantities σ(LLNL) and σ (ALS) are the rms residual height from the LLNL height and ALS slope measurements. Shaded area shows the difference between the measured height (LLNL) and the height generated (ALS) by integration in the frequency domain. The quantity $\sigma(\Delta)$ is the rms value of this difference.

Both of the methods described above for integration of slope data were applied and compared to measured height data from LLNL, for the HOMS-3 mirror. The results are summarized in Fig. 5, which shows the residual heights after

subtraction of the gravity sag and the best fitting parabola from each data set. The displayed data are only for the clear aperture of this mirror, spanning 380 mm and centered on the substrate's geometric center. In this particular case, the height calculated from slope data via the DFT as described above (blue dotted curve) and height calculated by a direct Riemann summation (red dashed curve) are practically indistinguishable. Moreover, there is good qualitative and statistical agreement between the measured height data obtained at LLNL (purple solid curve), and the height data generated from the ALS slope data. Both sets of measurements from LLNL and the ALS show a 1.9 nm root-mean-square (rms) variation of the residual height. In spite of the good qualitative agreement, the rms difference between the measurements is 1.5 nm. This is on the level of outstanding specifications for X-ray flat optics designed for free electron lasers.[4]

The parameters of second order polynomial fits of LLNL and integrated OML data differ by only 20%. Such a small difference indicates very good agreement between calibrations of LLNL and the ALS OML instruments. This is extremely important when curvatures are on the order of hundreds of kilometers.

Figure 6 shows the power spectral density (PSD) of the height data presented in Fig. 5. The overall shapes of the three PSDs are similar. For the low spatial frequencies ($\lesssim 0.02$ mm^{-1}), there is a good quantitative agreement. At higher spatial frequencies, the PSD of the height distribution measured with the interferometer is systematically higher of that of for the spectra generated from the slope data. This could be attributed to the fact that the technique of integration of a Fourier transform acts as a low-pass filter in the case of random noise.

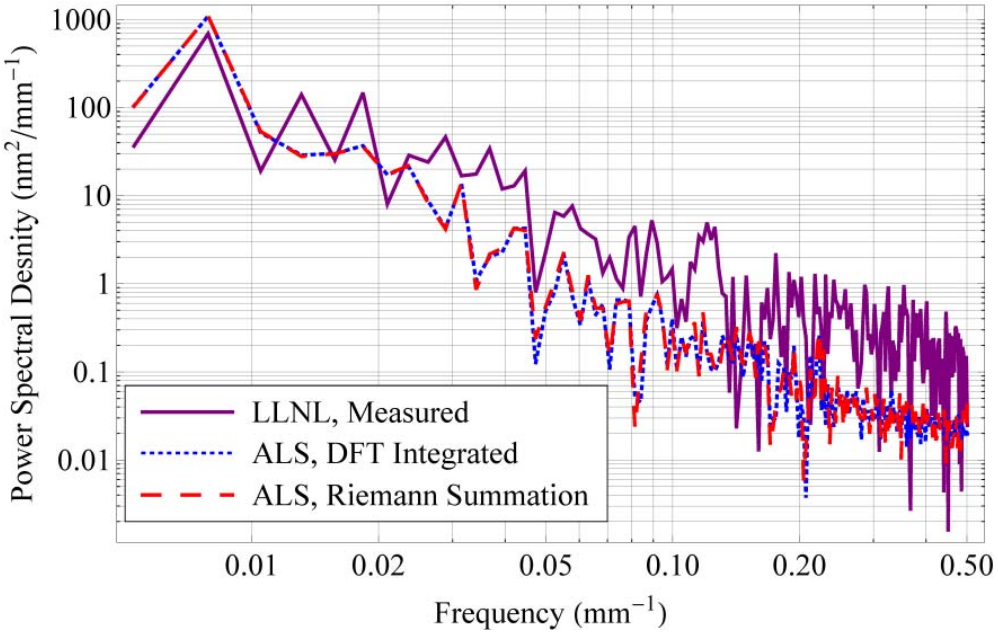

Figure 6: Power spectral densities (PSDs) the height data directly measured with the Fizeau interferometer and height data generated from slope data.

7. CONCLUSIONS

We have demonstrated that current state-of-the-art surface optical metrology is capable for precise characterization of surface figure of high quality x-ray optics designed and fabricated for FEL applications. The tested metrology methods are based on direct height measurements with a carefully calibrated Fizeau interferometer and on surface slope measurements utilizing sophisticated methods for suppression of the instrumental errors.

We have discussed in detail the methodology of transformation of the measured slope data into the surface height distributions. We have numerically shown that in our case the use of different integration methods leads to the indistinguishable height profiles. This can be an indication of a very small contribution of random error to the slope measurements. This conclusion is also confirmed by comparing the PSD spectra of the direct height data and the data obtained by integration of the measured slope profiles.

Note that the demonstrated accuracy of slope measurements on the level of 40-60 nrad rms has become possible due to averaging of multiple scans performed according to the optimal measuring strategies developed at the ALS OML.[16,19,20] Such multiple measurements require extended running time up to a few weeks. The running time is expected to be significantly shortened due to improvement of the OML environmental conditions. This work is in progress.

ACKNOWLEDGEMENTS

The Advanced Light Source is supported by the Director, Office of Science, Office of Basic Energy Sciences, Material Science Division, of the U.S. Department of Energy under Contract No. DE-AC02-05CH11231 at Lawrence Berkeley National Laboratory.

DISCLAIMER

REFERENCES

[1] The LCLS Design Study Group, “Linac coherent light source (LCLS) design study report,” SLAC-R-521.
[2] Boutet, S. and Williams, G. J., “The Coherent X-ray Imaging (CXI) instrument at the Linac Coherent, Light Source (LCLS),” New J. Phys. **12**(3), 035024 (2010).
[3] Maréchal, A., “Study of the combined effects of diffraction and geometrical aberrations on the image of a luminous point,” Rev. Opt. Theor. Instrum. 26, 257 (1947).
[4] Siewert, F., Buchheim, J., Boutet, S., Williams, G. J., Montanez, P. A., Krzywinski, J. and Signorato, R., “Ultra-precise characterization of LCLS hard Xray focusing mirrors by high resolution slope measuring deflectometry,” Opt. Express 20(4), 4525-36 (2012).
[5] Assoufid, L., Hignette, O., Howells, M., Irick, S., Lammert, H. and Takacs, P.Z., “Future metrology needs for synchrotron radiation grazing-incidence optics,” Nucl. Instr. and Meth. A 467-468, 267-70 (2001).
[6] Takacs, P. Z., “X-ray optics metrology,” Handbook of Optics, 3rd ed., Vol. V, M. Bass, Ed., Chapter 46, McGraw-Hill, New York (2009).
[7] Samoylova, L., Sinn, H., Siewert, F., Mimura, H., Yamauchi, K. and Tschentscher, T., “Requirements on Hard X-ray Grazing Incidence Optics for European XFEL: Analysis and Simulation of Wavefront Transformations,” Proc. SPIE 7360, 73600E-1-9 (2009).
[8] Siewert, F., Lammert, H. and Zeschke, T., “The Nanometer Optical Component Measuring Machine,” in [Modern Developments in X-ray and Neutron Optics], Erko, A.; Idir, M.; Krist, Th.; Michette, A.G. (Eds.), Vol. V, Springer, Berlin, Germany, 193-200 (2008).

[9] Alcock, S. G., Sawhney, K. J. S., Scott, S., Pedersen, U., Walton, R., Siewert, F., Zeschke, T., Senf, F., Noll, T. and Lammert, H., "The Diamond-NOM: A non-contact profiler capable of characterizing optical figure error with sub-nanometre repeatability," Nucl. Instr. and Meth. A, 616(2-3), 224-228 (2010).
[10] Senba, Y., Kishimoto, H., Ohashi, H., Yumoto,H., Zeschke, T., Siewert, F., Goto, S. and Ishikawa, T., "Upgrade of long trace profiler for characterization of high-precision X-ray mirrors at SPring-8," Nucl. Instr. and Meth. A, 616(2-3), 237-240 (2010).
[11] Rommeveaux, A., Hignette, O. and Morawe, C., "Mirror metrology and bender characterization at ESRF," Proc. SPIE 5921, 59210N 1-8 (2005).
[12] Rommeveaux, A., Thomasset, M. and Cocco, D., "The Long Trace Profilers," [Modern Developments in X-ray and Neutron Optics], A. Erko, M. Idir, T. Krist, A. G. Michette, Eds., Vol. V, Chapter 10, Springer, Berlin (2008).
[13] Thomasset, M., Brochet, S., Polack, F., "Latest metrology results with the SOLEIL synchrotron LTP,"Proc. SPIE 5921, 592102-1-9 (2005).
[14] Polack, F., Thomasset, M., Brochet, S., Rommeveaux, A., "An LTP stitching procedure with compensation of instrument errors: Comparison of SOLEIL and ESRF results on strongly curved mirrors," Nucl. Inst. and Meth. A, 616(2-3), 207-211 (2010).
[15] Kirschman, J. L., Domning, E. E., McKinney, W. R., Morrison, G. Y., Smith, B. V., and Yashchuk, V. V., "Performance of the upgraded LTP-II at the ALS Optical Metrology Laboratory," Proc. SPIE **7077**, 70770A-1-12 (2008).
[16] Yashchuk, V. V., Barber, S., Domning, E. E., Kirschman, J. L., Morrison, G. Y., Smith, B. V., Siewert, F., Zeschke, T., Geckeler, R., Just, A., "Sub-microradian Surface Slope Metrology with the ALS Developmental Long Trace Profiler," Nucl. Instr. and Meth. A, 616, 212-223 (2010).
[17] McKinney, W. R., Anders, M., Barber, S. K., Domning, E. E., Lou, Y., Morrison, G. Y., Salmassi, F., Smith, B. V., and Yashchuk, V. V., "Studies in Optimal Configuration of the LTP," Proc. SPIE 7801, 780106-1-12 (2010).
[18] McCarville, T., Soufli, R., Pivovaroff, M., "LCLS X-ray mirror measurements using a large aperture visible light interferometer," ACTOP11, 4th Workshop on Adaptive and Active X-ray & XUV Optics, 4th-5th April, Diamond Light Source, Oxfordshire, UK. (LLNL-CONF-472682), (2011).
[19] Ali, Z., Artemiev, N. A., Cummings, C. L., Domning, E. E., Kelez, N., McKinney, W. R., Merthe, D. J., Morrison, G. Y., Smith, B. V., and Yashchuk, V. V., "Automated suppression of errors in LTP-II slope measurements with x-ray optics," Proc. SPIE 8122, 8141-23 (2011).
[20] Yashchuk, V. V., "Optimal Measurement Strategies for Effective Suppression of Drift Errors," Rev. Sci. Instrum. 80, 115101-1-10 (2009).
[21] Savitzky, A., and Golay, M. J. E., "Smoothing and Differentiation of Data by Simplified Least Squares Procedures," *Analytical Chemistry*, 36, 1627–1639 (1964).
[22] Campos, J., Yaroslavsky, L. P., Moreno, A., and Yzuel, M. J., "Integration in the Fourier domain for restoration of a function from its slope: comparison of four methods," Optics Letters, 27(22), 1986-1988, (2002).